A Statistical Analysis of Expulsion Limits in Resistance Spot Welding

Hongyan Zhang
S. Jack Hu
Jacek Senkara[1]

Department of Mechanical Engineering and Applied Mechanics, University of Michigan, Ann Arbor, MI 48109

Shaowei Cheng
Department of Statistics, University of Michigan, Ann Arbor, MI 48109

Expulsion is an important phenomenon in resistance spot welding. It involves loss of metal from the liquid nugget, which often results in the reduction of weld strength. Various models have been proposed to understand expulsion mechanisms. In these models the occurrence of expulsion is often treated as a deterministic event, and depicted by a line (boundary) in conventional lobe diagrams. In this study, statistical analysis is employed to explore expulsion with consideration of the influence of random factors. Models are built based on experimental data, and one steel and two aluminum alloys are used as examples. Expulsion probabilities are presented as a function of electrode force, welding current, and time. Analytical models and their graphical form of expression (contours and surfaces) are created to present expulsion limits under various combinations of welding parameters. This study provides not only quantitative model predictions on expulsion limits for the materials studied, but also a generic statistical methodology that can be used for analyzing expulsion in various material systems. [S1087-1357(00)00602-X]

Introduction

As the predominant joining technique in sheet metal assembly, spot welding is widely used in manufacturing automobiles, airplanes, and appliances. One common phenomenon in spot welding is expulsion, the ejection of molten metal from the liquid nugget during welding. To achieve a weld size as large as possible to meet certain requirements, a prevalent practice is to use a large welding current, often close to expulsion settings. Expulsion limits are often deliberately exceeded in production to reduce variation in weld quality caused by random factors. However, because of the loss of metal during expulsion, defects, such as voids and porosity that may reduce weld strength, are introduced to the nugget. Expulsion also has negative influence on adhesive bonding, if it is used in conjunction with spot welding (so called weldbonding), by destroying adhesive layers. Therefore, it is crucial to control or eliminate expulsion, while maintaining sizable welds in resistance spot welding.

Expulsion is influenced by many factors of electrical, mechanical, thermal, and metallurgical nature. Most research activities are for expulsion detection only, as reviewed by Senkara et al. [1], and limited information can be obtained for expulsion control. Although there have been a number of attempts to predict expulsion, choosing correct welding schedules (usually electrode force, welding current, and welding time) is still the preferable way to control expulsion.

A common practice for determining a welding schedule is to find the limit of current for expulsion, with fixed electrode force and welding time. This is usually done using ''lobe'' diagrams (an example is shown in Fig. 1). Minimum acceptable weld sizes and expulsion limits, as functions of welding time and welding current, are the boundaries in a lobe diagram. To understand expulsion phenomenon and to predict expulsion limits, several theories or hypotheses on the causes of expulsion have been proposed. It was believed that electrode force causes expulsion, as stated by Davies [2]. The molten metal of a weld nugget is squeezed out by the electrodes, and expulsion happens. Excessive current density [3] or energy input [4] was also considered the reason for expulsion. The latest theory of expulsion is that it happens when the force from the nugget due to the internal pressure in a liquid nugget caused by melting, liquid expansion, and other factors exceeds the force from the electrodes [1]. Good agreement was achieved in experiments of an aluminum alloy using this theory. In addition to theories considering root causes of expulsion, there are also efforts to describe expulsion by mechanically comparing molten metal size with compressive zone size, as in the work by Browne et al. [5,6]. In all these models/theories welding time and current, or the formation process of weld nuggets, are not directly reflected. Intuitively, expulsion is determined by welding parameters, and how welding current and time interact with electrode force on expulsion is of practical significance in sheet metal assembly.

Weld lobes provide a simple way to understand the influence of welding parameters on expulsion limits. Most lobe diagrams are created using (single) fixed electrode force, while attempts with variable electrode forces have been made by several researchers. For instance, in the work by Schumacher and Soltis [7], 3-D weld lobes were created to describe the interactions of electrode force, welding current, and time. Similar work was done by Gould et al. [8] for resistance seam welding. Browne et al. [5,9] showed shifts of weld lobes or expulsion limits with electrode force in resistance welding an aluminum alloy, and their results are similar to those observed by Kaiser et al. [10] for welding low carbon and high strength-low alloy (HSLA) steels. Karagoulis [11] also reported weld lobe shifting due to electrode misalignment. But these works generally used a very limited number of electrode forces. This is partially because electrode force is believed to be less important than welding current and time, and partially due to the fact that the force is more difficult and tedious to change by using pneumatic cylinders. However, it is difficult to understand how welding parameters and their interaction influence the expulsion phenomenon from such analyses based on scattered data. On the other hand, the size of experiment matrix will be too large to handle if electrode force is taken as a variable in the same fashion as welding current and time.

Although expulsion can be accurately predicted by analyzing forces and sizes of the weldment during welding, as demonstrated in the work by Senkara et al. [1], it also involves many random factors that are difficult to detect. Examples of such random factors are worksheet fitup, electrode alignment (which often changes with electrode force), and contact resistance (which depends on

[1]On sabbatical leave from the Welding Department, Warsaw University of Technology, 85 Narbutta St., 02-524 Warsaw, Poland.

Contributed by the Manufacturing Engineering Division for publication in the JOURNAL OF MANUFACTURING SCIENCE AND ENGINEERING. Manuscript received Sept. 1998; revised Aug. 1999. Associate Technical Editor: E. C. DeMeter.

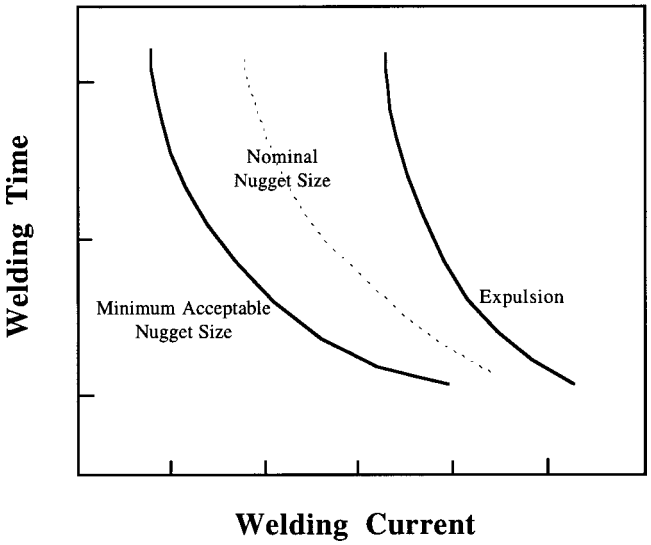

Fig. 1 A schematic ''lobe'' diagram. The electrode force is usually fixed.

electrode force, pressure distribution, and surface conditions). In order to link expulsion phenomenon directly to welding parameters, it is possible to incorporate the expulsion model [4] with finite element models which give accurate prediction of nugget size, such as the work by Browne et al. [5,6], Zhang et al. [12], and Gupta and De [13]. A shortcoming of such an approach is that the number of cases that can be simulated is quite limited, and the influence of random factors cannot be taken into account. In this study, a statistical analysis is performed to outline the expulsion limits based on experimental results. Unlike previous works on expulsion limits, explusion is not regarded as an event happening at a single welding schedule; rather, its occurrence is treated as a probability that spans from no expulsion to 100 percent of welds having expulsion with consideration of random factors. Predicting expulsion is useful in design and production where a certain percentage, rather than a definite number of conforming welds, is often more meaningful. First, in order to provide a methodology for investigating expulsion limits of various material systems, a detailed description of the statistical analysis is given in this paper, using welding a drawing steel (DS) as an example. The expulsion models of welding AA5754 and AA6111 are then presented. The results of the models are analyzed, and their implications in preventing expulsion by choosing correct welding parameters are discussed.

Experiment

One low-carbon bare steel (DS) and two aluminum alloys (AA5754 and AA6111) were used in the experiment. Welding schedules were chosen around potential expulsion boundaries, and adjustment on welding schedules was made during experiments according to previous observations, to effectively cope with the change of expulsion limits. In the experiments, welding current was varied for fixed electrode force and welding time. Different ranges of electrode force, welding current, and time were chosen for different materials. The occurrence of expulsion was clearly observed in the signals of dynamic resistance, secondary voltage, and the relative displacement between electrodes.

Steel. A DS bare steel of 1.2 mm gauge was used. Its chemical composition is shown in Table 1. A single-phase alternating current (AC) pedestal welder was used for welding. The experiments contained a large number of combinations of welding current, time, and electrode force. There were total 76 runs with 10 replicates each. Welding schedules are as follows.

Welding current (root-mean-square value, RMS): 6.5 to 13.9 kA (varied during welding);

Welding time: 133, 267, 400 ms (8, 16, 24 cycles);

Electrode force: 2.7, 3.6, 4.4, 5.3 kN (600, 800, 1000, 1200 lb).

Aluminum Alloys. Aluminum sheets of AA5754 (2.0 mm) and AA6111 (1.0 mm) were supplied by Alcan Aluminum Company, and treated by an Alcan surface treatment technique to ensure a repeatable surface condition. AA5754 is currently used for structural components, and AA6111 is used for enclosures in selected automobile models. The chemical compositions provided by the producer are listed in Table 2. A pinch gun with a medium frequency direct current (MFDC) transformer was used in the experiments. The welding parameters were chosen to cover a wide range of possibilities, they are

For AA5754, welding current: 20 to 35 kA (varied during welding);

Welding time: 67, 117, 167 ms (4, 7, 10 cycles);

Electrode force: 2, 3, 5, 7, 9 kN (450, 670, 1120, 1570, 2000 lb).

For AA6111, welding current: 5 to 40 kA (varied during welding);

Welding time: 20, 50, 75, 100 ms (1, 3, 4, 6 cycles);

Electrode force: 2, 4, 6 kN (450, 900, 1350 lb).

The experiments on AA5754 had 35 runs with 5 replicates each, and those on AA6111 had 132 runs with 5 replicates each.

Expulsion was monitored during welding. The occurrence of expulsion was calculated in terms of the percentage of welds with expulsion for a fixed welding schedule. The experimental results were then used in the statistical analysis and modeling of expulsion limits for these materials.

Statistical Analysis

Statistical analysis is ideal for welding research because of the multi-variable nature of welding processes. It provides a means to identify important factors and their interactions, and to develop statistical models (abbreviated as ''models'' hereafter) that can be used for predicting results or consequences, and for in-depth understanding of the physical processes involved. Because of the

Table 1 Chemical composition (wt.%) of the DS steel tested*

C	Mn	P	S	Si	Cu	Ni	Cr	Mo	Sn	Al	Ti
0.035	0.210	0.006	0.011	0.007	0.020	0.009	0.033	0.006	0.004	0.037	0.001

*Provided by National Steel Corp.

Table 2 Chemical compositions (wt.%) of commercial AA5754 and AA6111 alloys**

	Mg	Mn	Cu	Fe	Si	Ti	Cr	Zn
AA5754-O	2.6-3.6	<0.5	<0.1	<0.4	<0.4	<0.15	<0.3	<0.2
AA6111-T4	0.5-1.0	0.15-0.45	0.5-0.9	<0.4	0.7-1.1	<0.10	<0.10	<0.15

**Automotive Sheet Specification, 1994, Alcan Aluminum Company.

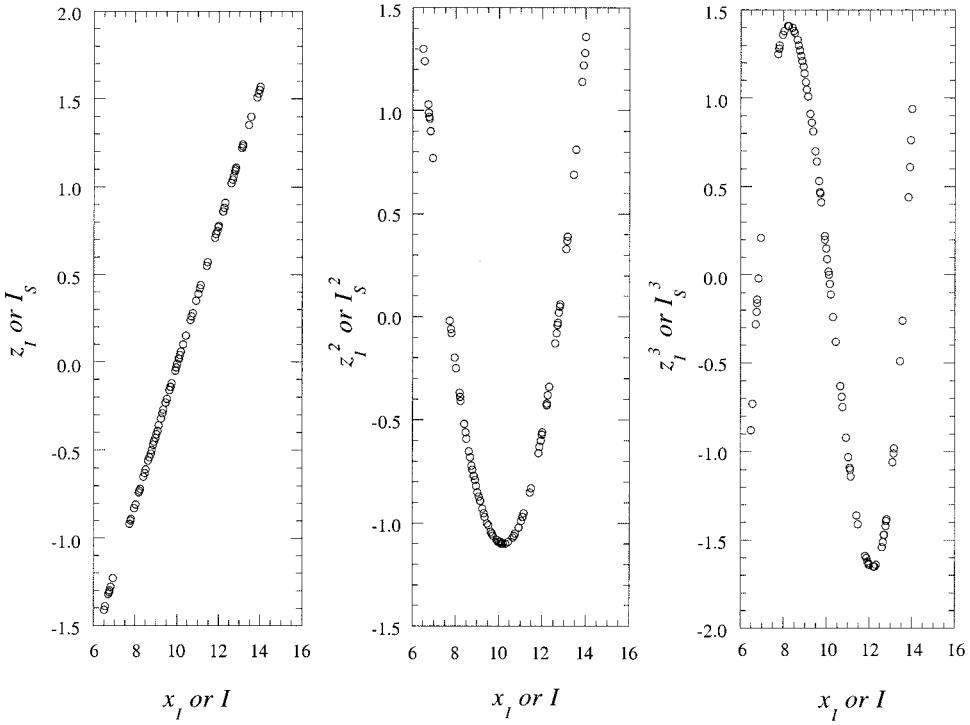

Fig. 2 Relationship between original current data and transformed (orthogonal) current data. From left to right: linear effect, quadratic effect, and cubic effect.

complex nature of expulsion, commonly used statistical procedures could not be directly applied, and certain modification had to be made in this study.

Modeling. The statistical model is for describing both the deterministic and random phenomena in expulsion experiment. In general, a model is often a function that can explain the relationship between input and output variables. Specifically, for this study, the model must be able to:

(a) explain and predict the frequency of occurrence of expulsion, using electrode force, current, and time;
(b) identify important effects and estimate their magnitudes;
(c) describe the randomness of occurrence of expulsion.

The statistical model chosen for this study is the frequently used logistic model, which is ideal for dealing with continuous input and output variables of count data. Details of the modeling are provided in the following sections.

The main purpose of this study is to understand the relationship between x (welding schedule) and p_x (probability of getting expulsion). In a logistic model, the common link function, which is used to describe the relationship between p_x and x, is as follows:

$$\mathrm{Log}(p_x/(1-p_x))=f(x) \tag{1}$$

$f(x)$ is a real function of x, and is usually approximated by the sum of polynomial terms of x. In this study there are three input variables: current (denoted by I), time (denoted by τ), and force (denoted by F), and $f(I,\tau,F)$ can be approximated as

$$\begin{aligned} f(I,\tau,F)\approx{}&\alpha_{000}+\alpha_{100}I+\alpha_{010}\tau+\alpha_{001}F+\alpha_{200}I^2+\alpha_{020}\tau^2+\alpha_{002}F^2\\ &+\alpha_{110}I\tau+\alpha_{101}IF+\alpha_{011}\tau F+\alpha_{300}I^3+\alpha_{030}\tau^3+\alpha_{003}F^3\\ &+\alpha_{210}I^2\tau+\alpha_{201}I^2F+\alpha_{021}\tau^2F+\alpha_{120}I\tau^2+\alpha_{102}IF^2\\ &+\alpha_{012}\tau F^2+\alpha_{111}I\tau F \end{aligned} \tag{2}$$

where α_{ijk}'s are the coefficients, usually called *parameters*, to be estimated using information from the data. Equation (2) is a 3rd order polynomial, and more terms can be chosen if more data is available. For details of logistic models, refer to the book by McCullagh and Nelder [14]. Experimental data needs to be transformed into a suitable form before performing statistical analysis. In this case, a coding system and pseudo data are needed.

Coding System and Transformations. In Eq. (2) $f(I,\tau,F)$ was expressed as the sum of polynomial terms of x's. However, the estimation of α_{ijk}'s may not be accurate due to co-linearity between polynomial terms. Hence, an orthogonal coding system is needed to translate polynomial vectors of x's into orthonormal vectors by the Gram-Schmidt process. The process is explained as follows:

Let $\mathbf{x_I},\mathbf{x_\tau},\mathbf{x_F}$ be the vectors which represent the data of current, time, and force, respectively, and let $\mathbf{x_I^2},\mathbf{x_\tau^2},\mathbf{x_F^2}$ be the vectors of taking the square of $\mathbf{x_I},\mathbf{x_\tau},\mathbf{x_F}$, and $\mathbf{x_I^3},\mathbf{x_\tau^3},\mathbf{x_F^3}$ of taking the cube of $\mathbf{x_I},\mathbf{x_\tau},\mathbf{x_F}$. Denote

$$\begin{aligned} u_I&=\mathbf{x_I}-(\mathbf{x_I}^T\mathbf{1})\mathbf{1}, \quad z_I=u_I/\|u_I\|\\ u_I^2&=\mathbf{x_I^2}-(\mathbf{x_I^2}^T z_I)z_I-(\mathbf{x_I^2}^T\mathbf{1})\mathbf{1}, \quad z_I^2=u_I^2/\|u_I^2\|\\ u_I^3&=\mathbf{x_I^3}-(\mathbf{x_I^3}^T z_I^2)z_I^2-(\mathbf{x_I^3}^T z_I)z_I-(\mathbf{x_I^3}^T\mathbf{1})\mathbf{1}, \quad z_I^3=u_I^3/\|u_I^3\| \end{aligned} \tag{3}$$

where $\mathbf{1}$ is the unit vector, $\mathbf{1}=(1,1,\ldots 1)$, and ''$T$'' indicates a transpose operation. z_I is called the linear effect of current, z_I^2 the quadratic effect of current, and z_I^3 the cubic effect of current. Figure 2 shows the relation between $\{z_I,z_I^2,z_I^3\}$ and original current data, $\mathbf{x_I}$. It is easy to see that $\{z_I,z_I^2,z_I^3\}$ are orthogonal with unit length. The same transformations are applied to $\{\mathbf{x_\tau},\mathbf{x_\tau^2},\mathbf{x_\tau^3}\}$ and $\{\mathbf{x_F},\mathbf{x_F^2},\mathbf{x_F^3}\}$. It can be proved that there is an one-to-one transformation between linear combination of polynomial terms of I's and that of I_S's, such as

$$\begin{aligned} I_s&=a_{10}+a_{11}I\\ I_s^2&=a_{20}+a_{21}I+a_{22}I^2\\ I_s^3&=a_{30}+a_{31}I+a_{32}I^2+a_{33}I^3 \end{aligned} \tag{4}$$

where a_{ij}'s are the transformation coefficients. Denote $\{I_s, I_s^2, I_s^3\}$ as the polynomials of $\{I, I^2, I^3\}$ under the same transformation as in Eq. (4). Applying similar transformations to time τ and force F, Eq. (2) can be rewritten as follows:

$$f(I,\tau,F) \approx \theta_{000} + \theta_{100}I_s + \theta_{010}\tau_s + \theta_{001}F_s + \theta_{200}I_s^2 + \theta_{020}\tau_s^2 + \theta_{002}F_s^2 + \theta_{110}I_s\tau_s + \theta_{101}I_sF_s + \theta_{011}\tau_sF_s + \theta_{300}I_s^3 + \theta_{030}\tau_s^3 + \theta_{003}F_s^3 + \theta_{210}I_s^2\tau_s + \theta_{201}I_s^2F_s + \theta_{021}\tau_s^2F_s + \theta_{120}I_s\tau_s^2 + \theta_{102}I_sF_s^2 + \theta_{012}\tau_sF_s^2 + \theta_{111}I_s\tau_sF_s \quad (5)$$

where θ_{000} is the coefficient of constant effect, θ_{100}, θ_{010}, and θ_{001} are coefficients of linear effects, θ_{200}, θ_{020}, and θ_{002} are of quadratic effects, θ_{300}, θ_{030}, and θ_{003} are of cubic effects. The subscripts denote the order of the input variables. Other θ_{ijk}'s are coefficients of interaction effects between I_s, τ_s, and F_s. Because polynomial terms of z's in the orthogonal coding system have better orthogonality property than those of x's, the estimators of coefficients in a model formed by polynomial terms of z's are more efficient and statistically independent. This makes a model selection procedure accurate, however, at the expense of losing intuitive physical interpretations of the coefficients. The fitted model using the orthogonal coding system can be transformed back to a function of x's with more meaningful coefficients. In this study, Eq. (5) was used to obtain a fitted model, and then it was transformed back to obtain a model of expulsion in the physical scale (Eq. (2)).

Use of Pseudo Data. The settings used in the steel welding experiment are shown in Fig. 3. It shows that the experiment region of welding current shifts to the right side when time decreases or force increases. Settings with low current and short time, as well as those with high current and long time were deliberately left out. The reason is that in those regions, expulsion either never happens (low settings) or always happens (high settings), and there is no need to conduct experiments at such settings. Such information that can be obtained without conducting an actual experiment is called ''prior knowledge.''

Although there is no need to conduct experiments, information in such regions is needed to build a statistical model. Bayesian approach is often employed to deal with prior knowledge, which is represented as distributions of coefficients. Because of the difficulty of translating the aforementioned prior knowledge of expulsion into distributions of coefficients, an alternative was adopted by using pseudo data to represent the prior knowledge. Twelve pseudo no-expulsion data were created on the low current side, and 12 expulsion data were created on the high current side. They are shown as solid dots in Fig. 3. Using a data set containing the pseudo data, the fitted model is able to represent the known information on expulsion.

Analysis and Results. In this section, the procedure of statistical analysis of expulsion is presented in detail, using the data of steel welding as an example.

Statistical Model Selection. It is quite often that only some of the effects are important and have significant influence on the output (probability of getting expulsion). Other insignificant effects can be screened out by means of model selection. Besides obtaining a model with only influential effects, another purpose of model selection is to get a balance between ''goodness-of-fit'' and

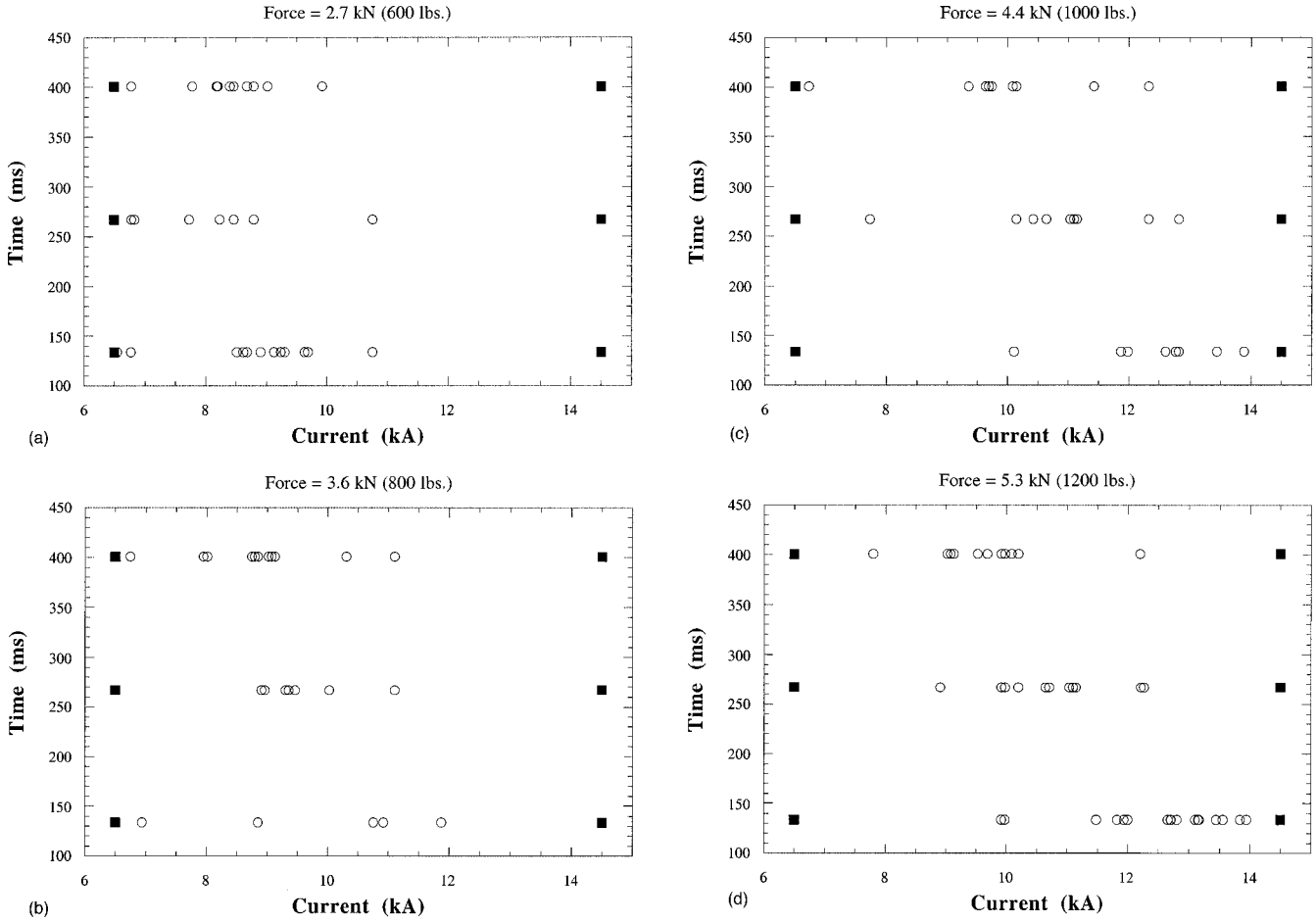

Fig. 3 Settings in the experiment of steel welding. Circles are experimental data, and solid squares are added pseudo data.

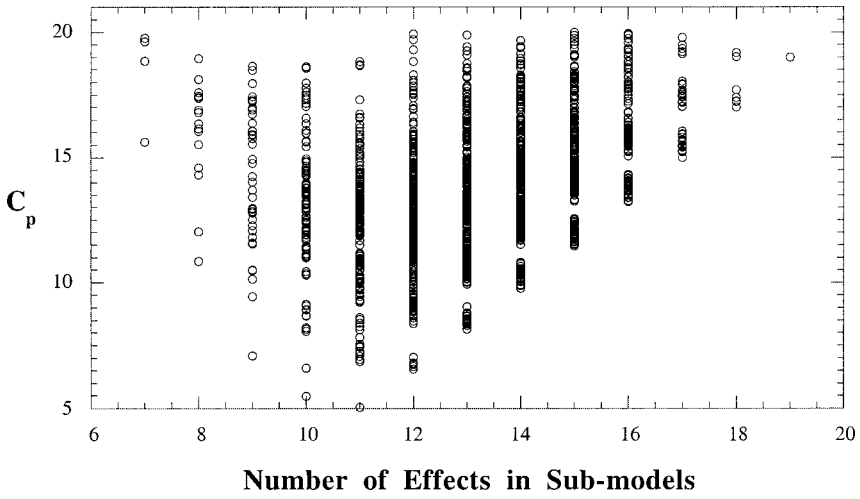

Fig. 4 A plot of C_p values versus the number of effects for the best sub-models

''generality.'' On one hand, having large effects in the fitted model can make it fit the data well in the regions where experimental data is available; therefore, it improves ''goodness-of-fit.'' On the other hand, the fitted model may be less able to be generalized to settings where no experimental data is available, i.e., it may not have ''generality.'' Hence, in order to keep good ''generality'' of a model, not too many effects should be included.

In this study, a criterion-based method was used for model selection. One of the commonly used criteria for general linear models, C_p criterion [15], was applied to each subset of the full model. This criterion is a measurement of both ''goodness-of-fit'' and ''generality.'' An appropriate model can be found by comparing the C_p value for each sub-model. The procedure of model selection is described as follows:

(a) Estimating p_x, the probability of getting expulsion on setting x, by y_x/n_x, the so-called observed p_x. n_x is the number of replicates, y_x is the number of expulsions observed on setting x, and y_x/n_x is the portion of the replicates in which expulsion happened. It is an intuitive estimation of p_x when no physical relationship is assumed between p_x and x.

(b) Transforming the logistic model (Eq. (1)) and replacing p_x in $\mathrm{Log}(p_x/(1-p_x))$ with y_x/n_x, and then denoting the logistic expression by w_x. To avoid divergence, 0.999 was used for $y_x/n_x=1$, and 0.001 was used for $y_x/n_x=0$. The vector of Eq. (5) can then be expressed as a general linear model:

$$\begin{aligned} w_x \approx\ & \theta_{000}+\theta_{100}z_I+\theta_{010}z_\tau+\theta_{001}z_F+\theta_{200}z_I^2+\theta_{020}z_\tau^2+\theta_{002}z_F^2 \\ & +\theta_{110}z_Iz_\tau+\theta_{101}z_Iz_F+\theta_{011}z_\tau z_F+\theta_{300}z_I^3+\theta_{030}z_\tau^3+\theta_{003}z_F^3 \\ & +\theta_{210}z_I^2z_\tau+\theta_{201}z_I^2z_F+\theta_{021}z_\tau^2z_F+\theta_{120}z_I\tau_\tau^2+\theta_{102}z_Iz_F^2 \\ & +\theta_{012}z_\tau z_F^2+\theta_{111}z_Iz_\tau z_F \end{aligned} \tag{6}$$

where w_x is called the dependent variable and $z_I, z_\tau, z_F, z_I^2, z_\tau^2, z_F^2, z_Iz_\tau, z_Iz_F, z_\tau z_F, \cdots$, are the independent variables in the general linear model.

(c) Applying model selection criteria to choose the best statistical model. The C_p criterion was then applied on dependent and independent variables. The formula for C_p criterion is as follows [15]

$$C_p=(RSS_p/\hat{\sigma}^2)+2p\text{-}n \tag{7}$$

where p is the number of effects in the model, n is the total number of settings, RSS_p is the residual sum of square calculated under this sub-model which contains p effects, and $\hat{\sigma}^2$ is the estimation of variance under the full model. The first part of the formula $(RSS_p/\hat{\sigma}^2)$ can be viewed as a measure of ''goodness-of-fit.'' $\hat{\sigma}^2$ is a constant over all sub-models. RSS_p is small if the fitted surface is close to y_x/n_x at experimental setting x. The rest of the formula, $2p\text{-}n$, is small if the number of effects in sub-models is small. Hence, a small C_p value is preferred. Fig. 4 shows how C_p values vary with the number of effects for the best sub-models. It can be seen that the C_p value first goes down then up when the number of effects in the sub-models increases, which means that the C_p criterion tries to get a balance between ''goodness-of-fit'' and ''generality.''

The model selection procedure described above is only based on statistics consideration. A model with a small C_p value may not be able to reflect the physical process. To overcome this, contour plots of fitted expulsion probability for a number of models with relatively small C_p values were compared. For example, Fig. 5 shows contour plots of two models of fitted expulsion probability created using this model selection process. Although both models have small C_p values, the trend shown in Fig. 5*b* is clearly contrary to, while the one in Fig. 5*b* is consistent with practical experience. Therefore, the model shown in Fig. 5*b* is a better choice.

By applying this model selection method to the data set for steel welding, a model was chosen in the orthogonal coding system, which contains linear, quadratic, and cubic effects, and their interactions: $z_I, z_\tau, z_F, z_\tau^2, z_F^2, z_I^3, z_F^3, z_\tau, z_F, z_Iz_F^2, z_I^2z_\tau, z_I^2z_F, z_\tau^2z_F$.

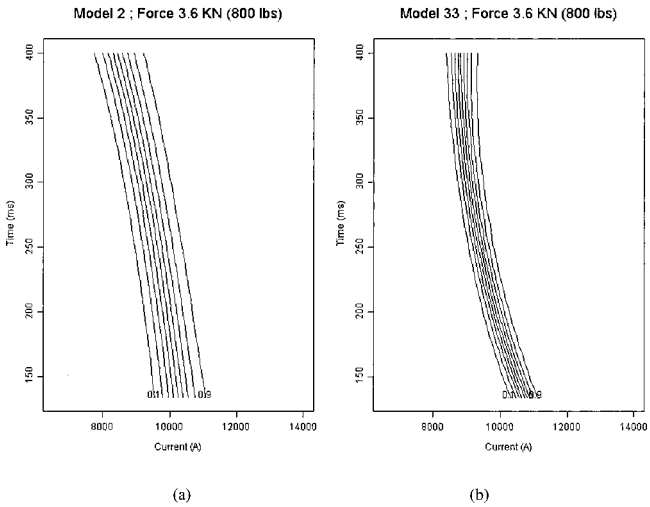

Fig. 5 Contours of two models with similar small C_p values

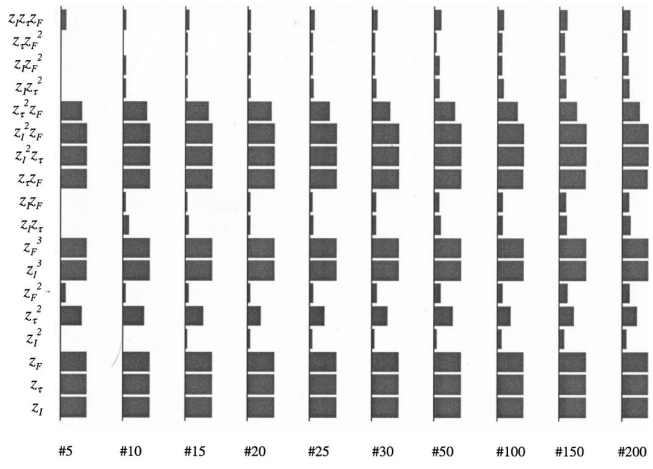

Fig. 6 Appearance frequency of effects in the first 5, 10, 15, 20, 25, 30, 50, 100, 150, and 200 ''best'' models

Identify Influential Effects. A model selected through previous steps usually contains many effects. Because of the co-linearity between effects, less important effects in the chosen model may be replaced by others, and the new model will still preserve the same ''goodness-of-fit.''

The results of model selection can help to identify important effects. Intuitively, if one effect has strong influence on the response, it should appear in most of the ''good'' models. Therefore, the frequency of each effect appearing in most of the ''best'' models was calculated, and effects with high appearance frequency were identified as influential effects (Fig. 6).

Eight effects were identified influential for the data set of steel welding: $z_I, z_\tau, z_F, z_I^3, z_F^3, z_\tau z_F, z_I^2 z_\tau, z_I^2 z_F$. They have frequencies of 1 from the beginning to the end, which means that they appear in all 200 ''best'' models. Besides, two other effects, z_τ^2 and $z_\tau^2 z_F$ also showed high frequency of appearance. It is noteworthy to see that all these 10 effects were included in the model identified in the previous model selection section.

Estimating Magnitudes of Effects. After choosing a statistical model by the model selection procedure described above, coefficients θ_{ijk}'s, the magnitudes of effects in the model can be estimated. For a logistic model, the estimation is proceeded by an iterative weighted least square procedure to get the maximum likelihood estimate of θ_{ijk}'s [14]. By doing this, coefficients of the steel welding model were estimated, and the model under orthogonal coding system can be expressed explicitly as follows:

$$\begin{aligned}\mathrm{Log}(p_x/(I-p_x)) \approx & (-9.037)+(38.360)I_s+(10.779)\tau_s \\ & +(-16.215)F_s+(-1.816)\tau_s^2+(1.385)F_s^2 \\ & +(3.645)\tau_s F_s+(6.236)I_s^3+(0.677)F_s^3 \\ & +(4.811)I_s^2\tau_s+(-8.253)I_s^2F_s \\ & +(-0.420)\tau_s^2F_s+(5.358)I_sF_s^2 \qquad (8)\end{aligned}$$

It can be transformed back to the coding system of true scale (with true values of welding current-kA, time-ms, and force-kN), as shown below:

$$\begin{aligned}\mathrm{Log}(p_x/(I-p_x)) \approx & (-7.6449\times10^2)+(1.6731824\times10^2)I \\ & +(7.12636\times10^{-1})\tau+(9.7174\times10^1)F \\ & +(-1.54168327\times10^1)I^2 \\ & +(-1.49\times10^{-5})\tau^2+(-4.234\times10^1)F^2 \\ & +(6.251982\times10^{-1})I^3+(1.4202468)F^3 \\ & +(-1.540455\times10^{-1})I\tau+(8.088965)IF \\ & +(6.08688\times10^{-2})\tau F+(7.5306\times10^{-3})I^2\tau \\ & +(-1.4449971)I^2F+(-5.12\times10^{-5})\tau^2F \\ & +(2.6919807)IF^2 \\ \equiv & f(I,\tau,F) \qquad (9)\end{aligned}$$

The fitted probability can be obtained by a simple transformation of above expression as:

$$p_x = e^{f(I,\tau,F)}/(1+e^{f(I,\tau,F)}) \qquad (10)$$

By standardizing the estimated coefficients in Eq. (9) with respect to their experimental ranges, and then comparing their magnitudes, the influential effects in the true scale were identified as (in the order of importance): I^2, I^3, I, I^2F, IF^2, $I\tau$, $I^2\tau$, F^2, IF.

After a statistical model is built, it needs to be judged by its closeness to the original data by using diagnostic methods, such as residual analysis, to see if there is any significant contradiction. Residual analysis on the model presented in Eq. (9) shows reasonable agreement between the observed and fitted values.

Models for Welding Aluminum Alloys. Following the statistical analysis procedure outlined above, experimental results on welding aluminum alloys were also analyzed, and the models created are shown in the following. For AA5754, the model is

$$\begin{aligned}\mathrm{Log}(p_x/(1-p_x)) \approx & (-2.372\times10^1)+(2.172\times10^1)I \\ & +(3.9\times10^{-3})\tau+(6.56\times10^{-1})F \\ & +(-2.79\times10^{-2})I^2+(-1.4\times10^{-3})I\tau \\ & +(-1.796\times10^{-1})IF+(-8.0\times10^{-4})\tau F \\ & +(2.7\times10^{-3})I^2F+(3.0\times10^{-4})I\tau F \\ \equiv & f(I,\tau,F) \qquad (11)\end{aligned}$$

The influential effects were identified as (in the order of importance): $I, F, IF, I^2, I^2F, \tau F$. For AA6111, the model is

$$\begin{aligned}\mathrm{Log}(p_x/(1-p_x)) \approx & (-1.394\times10^1)+(1.15\times10^1)I \\ & +(9.8\times10^{-2})\tau+(-3.15\times10^{-1})F \\ & +(-1.69\times10^{-2})I^2+(6.17\times10^{-2})F^2 \\ & +(-6.3\times10^{-3})I\tau+(-1.37\times10^{-1})IF \\ & +(1.0\times10^{-4})I^2\tau+(2.8\times10^{-3})I^2F \\ \equiv & f(I,\tau,F) \qquad (12)\end{aligned}$$

The influential effects are: $I, IF, I^2F, I\tau, I^2, I^2\tau$. It is noteworthy to see that models for AA5754 and AA6111 have very similar influential effects, which reveals the similarity in welding aluminum alloys.

Discussion

The statistical models shown in Eqs. (9), (11) and (12) represent the probability of expulsion as a continuous function of welding time, current, and force. There are a few observations that can be obtained by examining the results predicted by these statistical models.

Figure 7 shows a comparison of influential factors in steel and aluminum welding. The influence of a factor is represented by its relative value (percentage) in its own group of influential factors. Factors of values less than 5 percent are not presented. As shown in the figure, welding current related effects are most influential in both steel and aluminum welding, largely due to the fact that joule heating is the basis of resistance welding. Electrode force related

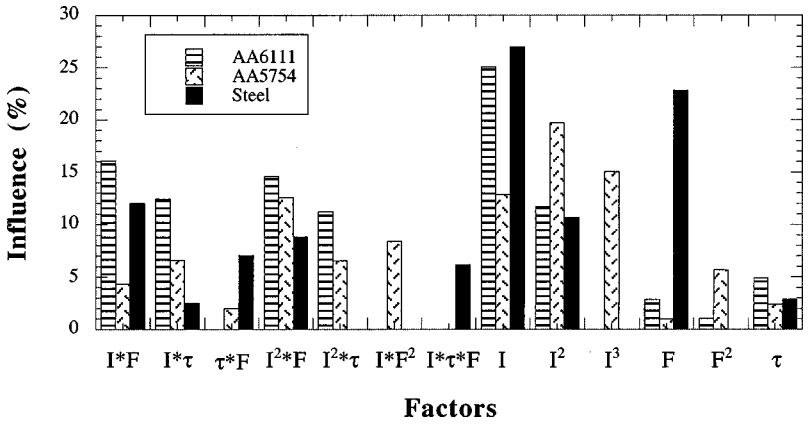

Fig. 7 A comparison of influencing factors in the models

effects are the second most influential in determining expulsion. This is especially true in steel welding. It is also interesting to see that welding time has the smallest influence.

3-D surface plots (generated using S-PLUS [16]) of the fitted p_x as a function of welding current and time are presented in Fig. 8. Because the electrode force is fixed, they can be regarded as 3-D lobe diagrams of expulsion. There are two plateaus in the surface plots for all three models. One is on the low setting side with probability of expulsion zero, and another on the high setting side with probability of one. Between these two there is a transition zone, in which the probability of expulsion changes continuously from zero to one. Therefore, an expulsion limit is not presented as a boundary or a line—as is done in most research work; rather it is presented as a range. Although weld lobes have been widely used for selecting welding parameters, there hasn't been a well-accepted means to determine expulsion boundaries. This is partially because there is no clear line between no-expulsion and expulsion. Because the occurrence of expulsion appears random in the transition region, it is reasonable and practical to treat expulsion statistically with occurrence probability.

The shape of expulsion probability surfaces (Fig. 8*a*) for the steel is also different from those of aluminum alloys (Figs. 8*b* and 8*c*). The figure shows that expulsion limits depend on welding time in steel welding, the same as observed experimentally by other researchers such as Kaiser et al. [10], while welding time is less influential for aluminum welding, similar to the observations by Browne et al. [5]. The transition from no-expulsion to expulsion appears smoother for AA6111 than for AA5754.

An obvious difference between expulsion limits of the steel and aluminum alloys is that expulsion boundaries (transition zones) of aluminum alloys are generally wider than those for the steel, which means that welding aluminum alloys has larger uncertainty in terms of expulsion. This can be seen more easily from the contour plots of expulsion probabilities of 0.05 and 0.95 generated using the models (Fig. 9). In the figure, expulsion boundaries move to the right side as electrode force increases. This phenomenon is similar to that observed by Kaiser et al. [10], and is consistent with the conclusions drawn by Senkara et al. [1], in which expulsion is directly linked to the effective electrode force.

The effect of electrode force is small for steel welding, but it is large for Al welding. This can be attributed to the fact that bulk resistance is dominant in steel, while surface resistance is dominant in Al welding. Electrode force or pressure has little if any, influence on bulk resistance, but significant effect on surface resistance. It is directly responsible for breaking aluminum oxide (Al_2O_3) layers on the surfaces of workpieces. Therefore, contact resistance, which provides most of the overall resistance in Al welding, is a strong function of electrode force. Figure 10 shows how total electrical resistance changes with electrode force in welding AA6111, using dynamic resistance signals recorded during experiments. It clearly shows that for the same welding time and current, larger electrode force results in lower total dynamic resistance in aluminum alloys by lowering surface resistance. Similar conclusions can be drawn from the work of Auhl and Patrick [17] and Patrick and Spinella [18] in their works on the influence of surface characteristics on aluminum welding. The aluminum welding experiments of this study also showed that expulsion behavior depends strongly on electrode conditions. All these factors contribute to the uncertainty, or wide ranges of expulsion probability in aluminum welding.

It's interesting to see the dependence of expulsion probability on welding force and current (Fig. 11), in addition to its dependence on welding current and time (Fig. 8). In general, expulsion depends on both electrode force and welding current. Treating electrode force as a continuous variable in the models enables a deep understanding of its influence on expulsion. An increase in electrode force reduces the chance of expulsion. However, the influence is a strong function of welding time for the steel, and a weaker function for Al alloys, as shown by the shape changes of surfaces in Fig. 11. Electrode force becomes less important for the steel welding when welding time is long. This is primarily due to the fact that the weld nugget size becomes influential, in addition to the electrode force, in controlling expulsion when the nugget size is close to the size of the electrode face after sufficient heating. The trends in surfaces of expulsion probability for AA5754 and AA6111 (Figs. 11*c–f*) are similar to those in the steel. Both electrode force and welding current affect expulsion probabilities with less magnitude than in the case of steel welding. Generally, the influence of welding time is very limited in Al welding, in consistence with the observation from Fig. 8. An examination of displacement signals shows that expulsion during Al welding often occurs at an early stage, and therefore, total set welding time has little effect.

The statistical models presented in this paper are important in understanding the complex phenomenon of expulsion in the steel and aluminum alloys studied. Although these models cannot be directly applied to other material systems, the methodology is generic. It is expected that different materials have different characteristics; therefore, they need different models of expulsion probability. Other factors such as the mechanical and electrical characteristics of a welding machine will also influence the expulsion models.

Summary

In this work, expulsion limits have been investigated statistically. Expulsion was treated as a phenomenon with probability of occurrence, unlike previous work on this topic. In summary, the following have been concluded in this study:

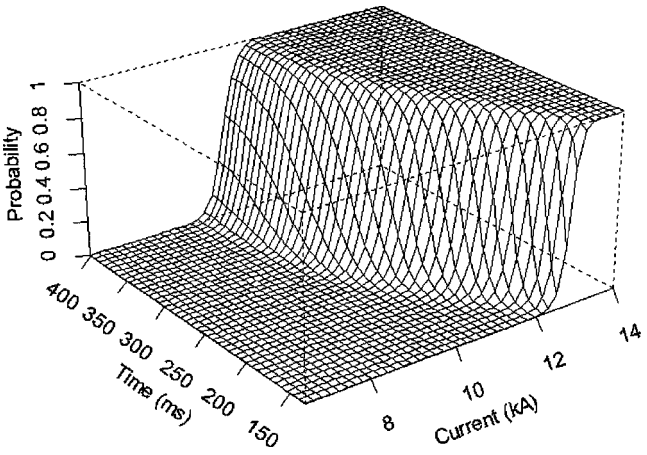

(a) DS steel. Force = 4.4 kN (1,000 lbs.)

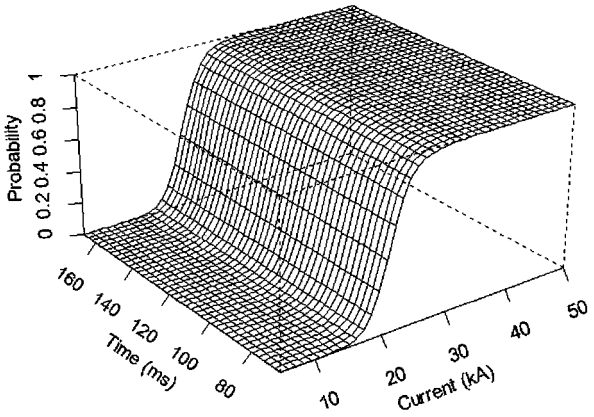

(b) AA5754. Force = 7kN (1,600 lbs.)

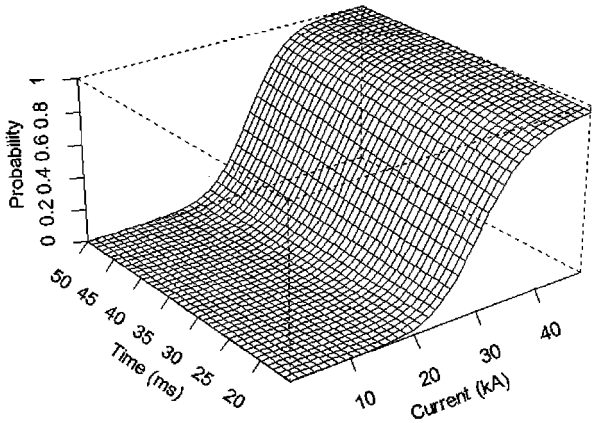

(c) AA6111. Force =3.6 kN (800 lbs.)

Fig. 8 Surface plots of expulsion probability at fixed forces

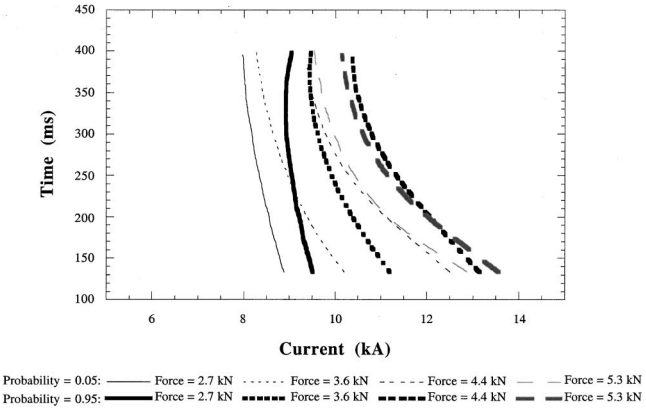

(a) DS steel.

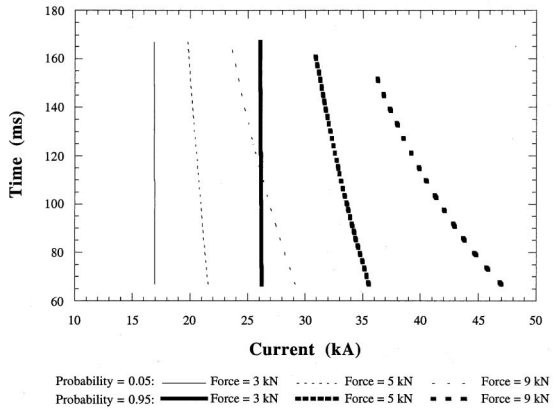

(b) AA5754.

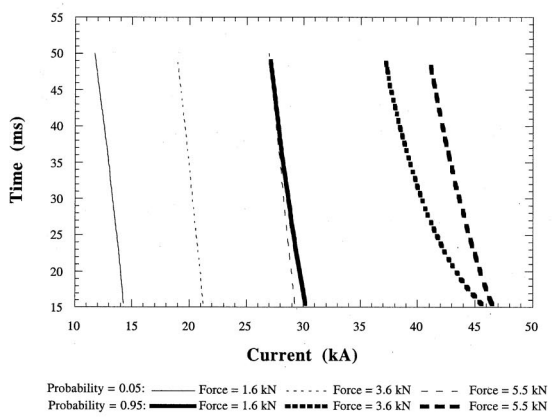

(c) AA6111.

Fig. 9 Contour plots of expulsion limits at various forces

• Statistical models have been developed, containing the effects of welding current, force, and time, and their interactions;

• Expulsion was treated as a dependent of both deterministic effects and random factors. Therefore, its boundary was determined as a probabilistic range, rather than a line;

• Welding current, time, and electrode force were all included in this study, unlike traditional lobe diagrams which are usually constructed using a fixed electrode force;

• The most influential welding parameter in determining expulsion is welding current for the steel and aluminum alloys. Electrode force is the second most important factor, while welding time is the least influential.

The methodology developed in this paper can be used to study expulsion in various material systems. The concept of expulsion probability provides a quantitative guideline and the potential to have a better control of resistance weld quality, by allowing the largest possible spot welds without expulsion.

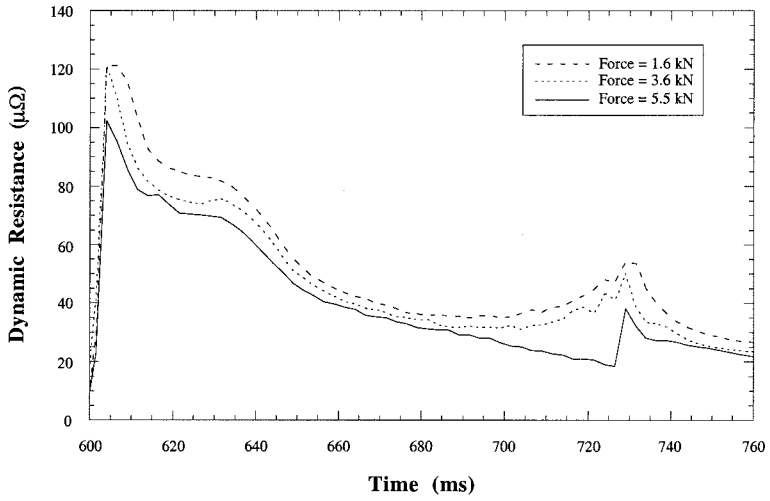

Fig. 10 Dynamic resistance versus welding time for AA6111. Welding time and current were the same while electrode force was altered.

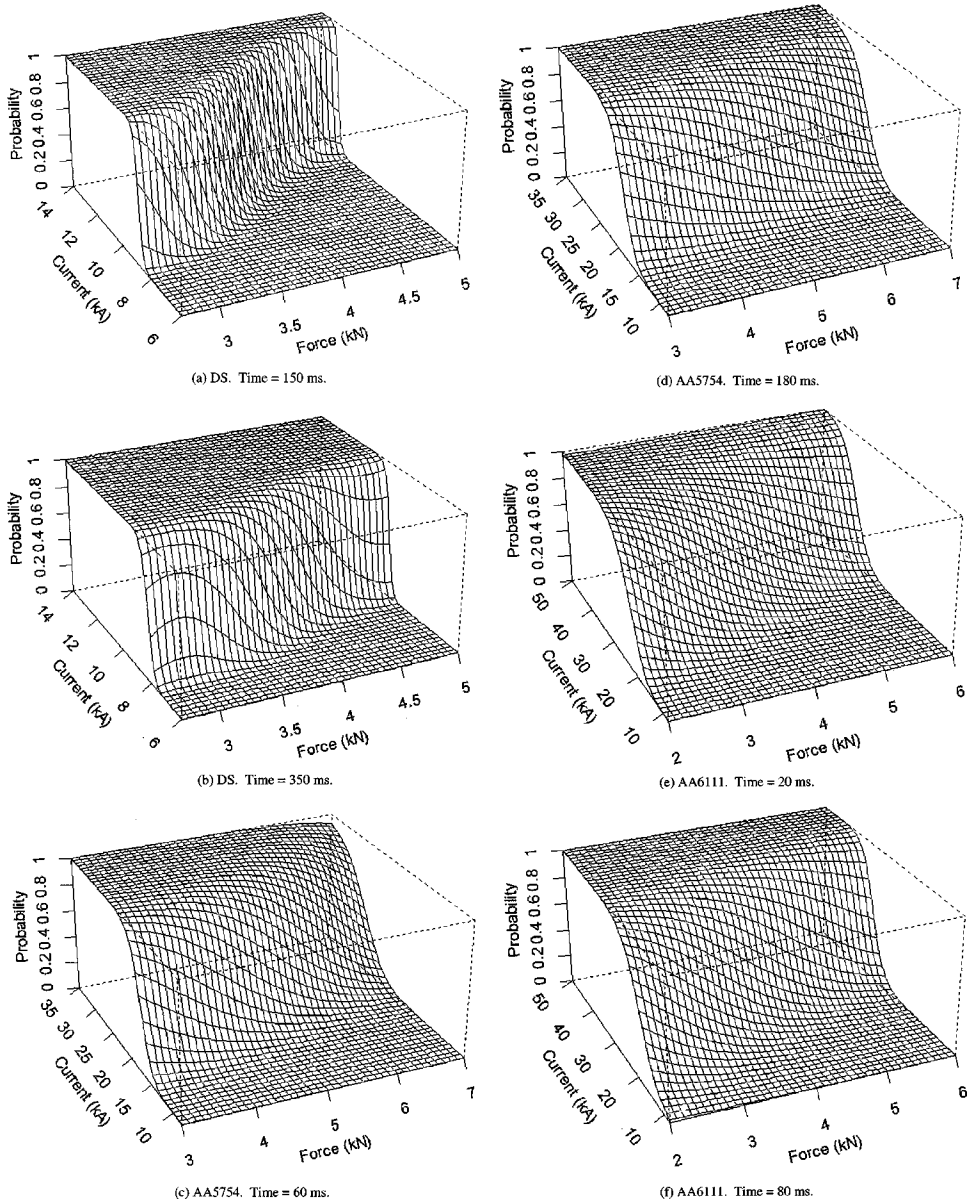

Fig. 11 Expulsion probability versus welding current and electrode force

Acknowledgment

The authors would like to thank Mr. Douglas R. Boomer of Alcan Aluminum Company for providing the aluminum alloys for testing, and to Mr. Matt Takahashi of National Steel Corp. for providing the steel and conducting chemical analysis. The authors are also grateful to the financial support of this work by the Advanced Technology Program (ATP/NIST) through the Intelligent Resistance Welding Consortium.

References

[1] Senkara, J., Zhang, H., and Hu, S. J., 2000, ''Expulsion Prediction in Resistance Spot Welding,'' Welding J., in press.
[2] Davies, A. C., 1993, ''The Science and Practice of Welding: Volume 2—The Practice of Welding,'' 10th ed., p. 210.
[3] Wu, K. C., 1977, ''The Mechanism of Expulsion in Weldbonding of Anodized Aluminum,'' Weld. J. (Miami), **56**, No. 8, pp. 238-s to 244-s.
[4] Dickinson, D. W., Franklin, J. E., and Stanya, A., 1980, ''Characterization of Spot Welding Behavior by Dynamic Electrical Parameter Monitoring,'' Weld. J. (Miami), **59**, No. 6, pp. 170-s to 176-s.
[5] Browne, D. J., Chandler, H. W., Evans, J. T., and Wen, J., 1995, ''Computer Simulation of Resistance Spot Welding in Aluminum-Part I,'' Weld. J. (Miami), **74**, No. 10, pp. 339-s to 344-s.
[6] Browne, D. J., Chandler, H. W., Evans, J. T., James, P. S., Wen, J., and Newton, C. J., 1995, ''Computer Simulation of Resistance Spot Welding in Aluminum-Part II,'' Weld. J. (Miami), **74**, No. 12, pp. 417-s to 422-s.
[7] Schumacher, B. W., and Soltis, M., 1988, ''Getting Maximum Information from Welding Lobe Tests,'' *Proc. AWS Sheet Metal Welding Conference III*, Detroit, Mich., Paper No. 16.
[8] Gould, J. E., Kimchi, M., Leffel, C. A., and Dickinson, D. W., 1991, ''Resistance Seam Weldability of Coated Steels. Part I: Weldability Envelopes,'' Edison Welding Institute Research Report, MR9112, Nov. 1991.
[9] Browne, D. J., Newton, C., and Boomer, D. R., 1995, ''Optimization and Validation of a Model to Predict the Spot Weldability Parameter Lobes for Aluminum Automotive Body Sheet,'' *Proc. International Body Engineering Conference IBEC'95-Advanced Technologies & Processes*, pp. 100–106.
[10] Kaiser, J. G., Dunn, G. J., and Eagar, T. W., 1982, ''The Effect of Electrical Resistance on Nugget Formation During Spot Welding,'' Weld. J. (Miami), **61**, No. 6, pp. 167-s to 174-s.
[11] Karagoulis, M. J., 1992, ''Control of Materials Processing Variables in Production Resistance Spot Welding,'' *Proc. AWS Sheet Metal Welding Conference V*, Detroit, Mich., Paper No. B5.
[12] Zhang, H., Huang, Y., and Hu, S. J, 1996, ''Nugget Growth in Spot Welding of Steel and Aluminum'' *Proc. AWS Sheet Metal Welding Conference VII*, Detroit, MI, Paper No. B3.
[13] Gupta, O. P., and De, A., 1998, ''An Improved Numerical Modeling for Resistance Spot Welding Process and Its Experimental Verification,'' ASME J. Manuf. Sci. Eng., **120**, pp. 246–251.
[14] McCullagh, P., and Nelder, J. A., 1989, *Generalized Linear Models*, 2nd ed., Chapman & Hall, London, UK, pp. 21–135.
[15] Sen, A., and Srivastava, M., 1990, *Regression Analysis: Theory, Methods, and Applications*, Springer-Verlag, New York, pp. 234–238.
[16] S-PLUS, Version 3.4 for Sum SPARC. Copyright 1996, MathSoft, Inc.
[17] Auhl, J. R., and Patrick, E. P., 1994, ''A Fresh Look at Resistance Spot Welding of Aluminum Automotive Components,'' SAE Paper No. 940160.
[18] Patrick, E. P., and Spinella, D. J., 1996, ''The Effects of Surface Characteristics on the Resistance Spot Weldability of Aluminum Sheet,'' *Proc. AWS Sheet Metal Welding Conference VII*, Troy, Mich., Paper No. B4.